AlN/GaN double-barrier resonant tunneling diodes grown by metal-organic chemical vapor deposition

C. Bayram, Z. Vashaei, and M. Razeghi[a)]
Department of Electrical Engineering and Computer Science, Center for Quantum Devices, Northwestern University, Evanston, Illinois 60208, USA

(Received 23 November 2009; accepted 29 December 2009; published online 25 January 2010)

AlN/GaN double-barrier resonant tunneling diodes (RTDs) were grown by metal-organic chemical vapor deposition on sapphire. RTDs were fabricated via standard processing steps. RTDs demonstrate a clear negative differential resistance (NDR) at room temperature (RT). The NDR was observed around 4.7 V with a peak current density of 59 kA/cm^2 and a peak-to-valley ratio of 1.6 at RT. Dislocation-free material is shown to be the key for the performance of GaN RTDs. © *2010 American Institute of Physics*. [doi:10.1063/1.3294633]

The resonant tunneling diode[1] (RTD) is a quantum-effect device that has attracted considerable attention because of its strong negative differential resistance (NDR) at room temperature (RT) and its high-speed switching and oscillation characteristics associated with NDR effect. Various material systems [such as AlGaAs/GaAs (Ref. 1) and InAs/AlSb (Ref. 2)] have been used to fabricate RTDs. The properties of nitride materials (AlGaInN) such as high peak electron velocity, saturation velocity, and thermal stability appeal for RTD applications. Specifically, AlN/GaN RTDs are expected to have higher peak-to-valley ratio (P/V) and operation at RT due to larger conduction band discontinuity (~2.1 eV) at AlN/GaN heterointerface.[3] Thus, these RTDs can be operated in terahertz regime at RT enabling many applications such as ultraspeed wireless communications, spectroscopy, and imaging. However, scattering and space charge effects are significant deterrents to NDR. For III-Nitrides, polarization charges as well as large lattice mismatch (and associated dislocations) also come into play making the observation of tunneling phenomena even more challenging.[4]

First works on III-Nitride RTDs has led debatable results with low reproducibility and stability.[5,6] Previous works report RTDs with P/V from 32 (for AlN/GaN heterostructure on sapphire)[7] to 2 (for $Al_{0.7}Ga_{0.3}N/GaN$ heterostructure on free-standing c-GaN).[8] However, these RTDs were grown by molecular beam epitaxy (MBE), and no studies yet can demonstrate RT NDR at RTDs grown by metal-organic chemical vapor deposition (MOCVD). A recent vertical transport study demonstrates NDR in Schottky device at cryogenic temperatures[9] motivating MOCVD-grown RTDs for RT operation. Today, most nitride based commercial optoelectronic devices are grown by MOCVD. Thus, there is a wide interest to study and demonstrate NDR and RTDs by MOCVD.

We have recently shown high quality AlN/GaN and $Al_{0.2}Ga_{0.8}N/GaN$ superlattices (SLs) with intersubband absorption at optical communication wavelengths (~1.5 μm) (Refs. 10 and 11) and at mid-infrared (~5.3 μm), respectively.[12] All these results were realized by MOCVD demonstrating unique capabilities of abrupt Al(Ga)N/GaN interfaces with MOCVD. In our earlier work,[13] we introduced a five-step lateral epitaxial overgrowth (LEO) GaN growth process that minimized dislocations in the wing regions of LEO GaN. This improved LEO GaN template enabled higher performance visible light emitters.[13] In this work, we utilized our high quality LEO GaN as a template in our AlN/GaN double barrier (DB) RTDs. RTDs with mesa size of 5 μm diameter were fabricated and their NDR characteristics and their dependence on the relative template location (on the wing and/or opening regions) were studied. P/V comparable to MBE-grown RTDs on free-standing GaN substrates[8] was realized on sapphire substrates by MOCVD.

The material was grown in an AIXTRON 200/4-HT horizontal flow low-pressure MOCVD reactor. Trimethylaluminum and trimethylgallium were used as the metalorganic precursors for Al and Ga, respectively. Silane was used as the *n*-type dopant source. Ammonia and hydrogen were used as the anion source and carrier gas, respectively.

First, the template, consisted of a high-quality LEO GaN, was grown on double-side polished (001) sapphire.[13] The LEO GaN employed a 15 μm period with a 2 μm opening leading to a dislocation-minimized wing region of 6.5 μm [Figs. 1(a) and 1(b)]. In order to study the dislocations, a hot phosphoric acid (85% H_3PO_4) treatment for 15 min was used. This etch-pit-density (EPD) study reveals no discernable dislocations in the wing areas of LEO GaN, whereas in the LEO GaN coalescence area and opening region dislocations of $(2\pm1)\times10^8$ and $(9\pm2)\times10^8$ cm^{-2} are observed, respectively, as shown in Fig. 1(a).

A typical (5×7 μm^2) atomic force microscope (AFM) scan of the LEO GaN template region is shown in Fig. 1(b). The wing region [Fig. 1(b)], where lateral growth occurs, possesses well-ordered parallel atomic steps with no atomic step terminations, and (5×5 μm^2) region has a root-mean-

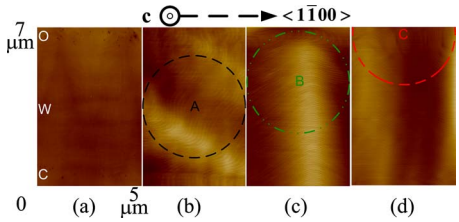

FIG. 1. (Color online) (5×7 μm^2) AFM images of (a) EPD study of LEO GaN, (b) LEO GaN template, (c) RTD active layer, and (d) completed RTD structure. The letters "O," "W," and "C" stands for opening, wing, and coalescence regions of the LEO GaN. Circles A, B, and C denotes the relative location of RTD devices A, B, and C.

a)Electronic mail: razeghi@eecs.northwestern.edu.

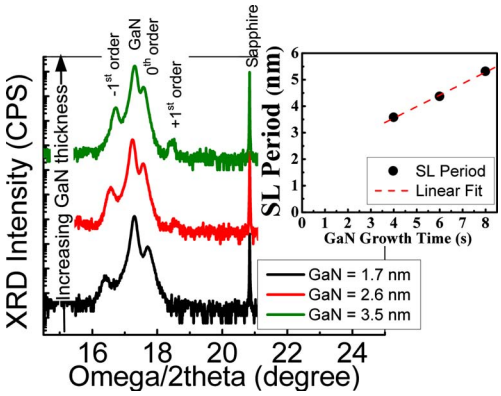

FIG. 2. (Color online) MOCVD growth calibration of the RTD active layer. X-ray diffraction of fifty periods of AlN/GaN SLs with different (1.7, 2.6, and 3.5 nm) GaN thicknesses (for a constant AlN thickness of 1.9 nm) are shown. The inset shows the SL period with respect to GaN growth time.

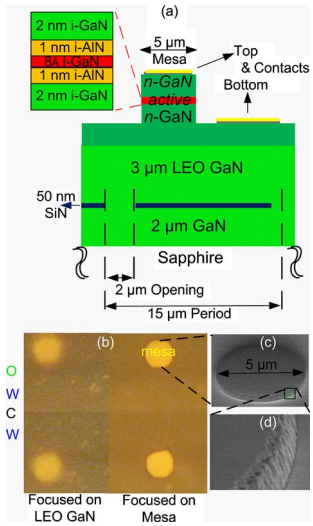

FIG. 3. (Color online) (a) The schematic view of the RTD, (b) the optical microscope image (focused on LEO GaN template and RTD mesa). The letters "O," "W," and "C" stands for opening, wing, and coalescence regions of the LEO GaN. (c) SEM image of an RTD mesa, and (d) SEM image of an RTD sidewall, top and bottom areas.

square (RMS) roughness of 1.7 Å. Then 500 nm thick *n*-GaN (with a carrier concentration of 4×10^{18} cm^{-3}) was regrown at 100 mbar on this coalesced LEO GaN to act as the *n*-contact region of RTD.

The active layer of the RTD, composed of AlN/GaN heterointerface, was first calibrated by growing AlN/GaN SLs on 2 μm thick GaN on sapphire at a pressure of 50 mbar. Via varying the deposition time of GaN (AlN) while keeping the AlN (GaN) deposition time constant, fifty periods of various SL samples were grown (see Fig. 2), and layer thicknesses were deducted.[10,11] The omega/2theta x-ray diffraction scans of three calibration SLs composed of 1.7, 2.6, and 3.5 nm thick GaN (and all employing 1.9 nm thick AlN) are given in Fig. 2. Figure 2 inset displays the SL period as a function of GaN deposition time. Under these MOCVD growth conditions, no significant GaN-thinning was observed. This was due to employing lower growth temperature to minimize aluminum adatom etching effect on gallium ones.[11] The growth rates of AlN and GaN were determined as 0.33 and 4.34 Å/sec, respectively. Based on these extracted growth rates, the active layer composed of (2 nm *i*-GaN/1 nm *i*-AlN/8 Å *i*-GaN/1 nm *i*-AlN/2 nm *i*-GaN) was regrown on *n*-GaN. The undoped 2 nm *i*-GaN was inserted before and after the DB AlN/GaN layer to act as spacer layers between highly doped bottom and top contact layers and undoped DB layer.

This active layer was capped with 300 nm *n*-GaN to form the top *n*-contact region, under the same growth conditions of bottom *n*-contact region. Typical (5×7 μm^2) AFM images of the active layer surface and the completed RTD surface on wing region are given in Figs. 1(c) and 1(d). The smooth sawtoothlike atomic steps are observed on wing area whereas chaotic atomic steps are recognized for the opening area. AFM scans of (5×5 μm^2) wing area possess RMS roughness of 1.3 and 1.1 Å for active layer surface and completed RTD surface, respectively. RTD device [device A in Fig. 1(b)] fabricated on this wing region is sketched in Fig. 3(a).

Device fabrication was realized via standard semiconductor processing techniques. First, the surface was dry-etched 50 nm with $SiCl_4$-based chemistry by electron cyclotron resonance reactive ion etching (ECR-RIE), and contact metal of 40 nm Ti/120 nm Au was deposited by electron beam (e-beam) evaporation. Then, 5 μm diameter mesas were defined by standard lithography thereafter by ECR-RIE. The mesa formation of the RTD was realized in two steps. The first step was the etching of the deposited top metal contact via CH_4-based chemistry. Then the sample was taken out so that the ECR-RIE system could be seasoned and tested, and the second etching step was realized; etching of the (Al)GaN layers via $SiCl_4$-based chemistry.[14] After proper sample cleaning, the bottom contact metal of 40 nm Ti/120 nm Au was deposited by e-beam evaporation. The Ohmicity of the bottom and top contacts were verified via independent transmission line measurement studies.

Figure 3(a) displays the sketch of the fabricated RTD. Figure 3(b) shows the fabricated RTDs under optical microscope. As there is ~4 μm vertical separation between LEO GaN pattern and the top metal contact, the optical microscope was focused on LEO GaN [Fig. 3(b) left] and mesa [Fig. 3(b) right] for the same device to demonstrate alignment of RTD mesas with respect to LEO GaN wing region (see Fig. 1). Figure 3(c) shows the scanning electron microscope (SEM) image of a single RTD mesa. Figure 3(d) illustrates the side wall profile of the RTD mesa. Due to employment of two-step dry-etching with two different chemistries,[14] the metal top contact was slightly underetched giving a good metal coverage on the mesa.

RT current-voltage (I-V) characteristics were obtained by probing the device. The voltage polarity refers to that applied to the top electrode. I-V curves were measured using an HP4155A Semiconductor parameter analyzer configured to input a voltage sweep while measuring current. Figure 4 shows RT I-V curves of three RTDs (designated by A, B, and C) taken by sweeping the voltage from −2 up to 8 V while measuring the current through the device. Device A was the RTD centered on the wing region, B was the neighbor of A closer to opening, and C was the neighbor of B toward opening (Fig. 1). For device A, we observed a clear NDR at 4.7 V with a peak current density around 59 kA/cm^2 and a peak-to-valley ratio of about 1.6 at RT. There were multiple data points taken in the NDR regime showing the clear decrease in current as the voltage was increased. The neighboring device, B, also demonstrated a clear NDR at 6.0 V with a peak current density around 120 kA/cm^2 and a peak-to-valley ra-

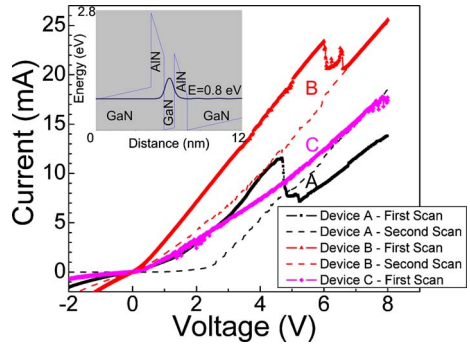

FIG. 4. (Color online) RT I-V curves, taken by sweeping voltage in positive direction while measuring current, of RTDs. Device A is on the wing where as from B to C mesa gets closer to opening (see Fig. 1). Inset displays the schematic conduction band diagram of DB active layer.

tio of about 1.2 at RT. However, the significant increase in NDR voltage (V_{NDR}) and decrease in P/V just moving slightly from wing toward opening were noticeable. The dependence of the V_{NDR} and P/V on the surface roughness was very strong, as can be seen from Fig. 4, resulting in doubling of peak current for diodes having some parts on opening. Interface-roughness/island scattering reduces the P/V and increases the valley current than the perfect planar case for AlGaAs/GaAs RTDs.[15] Considering the strong polarization in III-nitrides, effect of interface roughness is expected to be more important. This surface effect on RTD performance was observed more dominantly in device C. Most devices that have parts on the opening such as device C, did not demonstrate any NDR. This suggests that RTDs are very sensitive to surface roughness and dislocations, and NDR can be observed only on a very high quality template with a very high quality active layer (refer to Fig. 1 to compare the surface quality and dislocation density of device A, B, and C). Based on our EPD studies, the density of dislocations within RTDs A, B, and C are estimated as $\ll 10^7$, $(2\pm1)\times10^7$, and $(2\pm1)\times10^8$ cm^{-2}, respectively. This result demonstrates the importance of dislocation-free templates and the quality of the epitaxial growth, and may explain the nonreproducibility of the some group's results by other groups. The observed asymmetry of the I-V characteristics with respect to the applied voltages was caused by an asymmetry of the barrier structure caused by the polarization charges at the heterointerfaces in the DB region.[16,17] These charges also led to NDR for one bias polarity and not for the opposite one, in harmony with the theory[17] and our observations.[7,8]

Figure 4 inset displays the simulated[12] schematic conduction band diagram of DB active layer. The expected V_{NDR} was ~1.6 V. The relatively large observed V_{NDR} in our device were attributed to a small series resistance that becomes relatively important at high currents. In addition, polarization field was reported to shift the energy of the transmission peak with respect to one which could be obtained in absence of the field.[3,4] This suggests further improvements in material growth and device fabrication are necessary for optimal performance.

The NDR degraded for the consecutive I-V curve scan (Fig. 4). A strong hysteresis and the degradation in NDR were previously reported for RTDs both on sapphire[7] and on free-standing GaN substrate.[8] Hysteresis loop is more pronounced in III-nitrides and observed at RT due to a wide energy gap, large energy values of band and effective mass discontinuities, and the effect of built-in fields.[18] Thus, we attribute the degradation of the NDR for the consecutive scan to strong hysteresis and bias-dependent trapping of electrons, possibly assisted by strong polarization fields.[8,18] The consecutive scan possessed a lower current under reverse bias (Fig. 4). This could be related to change in the current formation mechanism as predicted in theory[19] and reported experimentally.[6]

In conclusion, we have demonstrated RT NDR in AlN/GaN DB-RTDs on LEO GaN templates grown by MOCVD. Peak-to-valley ratio of about 1.6 was achieved for RTDs aligned on the wing region at RT. The NDR was shown to be very sensitive to dislocations and surface roughness, and to degrade when RTD mesas did not align on wings. P/V comparable to MBE-grown RTDs on free-standing GaN substrates[8] was realized on sapphire substrates by MOCVD. MOCVD was shown to be capable of achieving very high quality AlN and GaN epitaxial surfaces, and of growing RTDs for RT III-nitride tunneling studies.

The authors acknowledge Dr. J. Zavada of ARO and Dr. J. Mangano of DARPA for their interest and encouragement.

[1]L. L. Chang, L. Esaki, and R. Tsu, Appl. Phys. Lett. **24**, 593 (1974).
[2]E. R. Brown, T. C. L. G. Sollner, C. D. Parker, W. D. Goodhue, and C. L. Chen, Appl. Phys. Lett. **55**, 1777 (1989).
[3]F. Sacconi, A. D. I. Carlo, and P. Lugli, Phys. Status Solidi A **190**, 295 (2002).
[4]M. Hermann, E. Monroy, A. Helman, B. Baur, M. Albrecht, B. Daudin, O. Ambacher, M. Stutzmann, and M. Eickhoff, Phys. Status Solidi C **1**, 2210 (2004).
[5]C. T. Foxon, S. V. Novikov, A. E. Belyaev, L. X. Zhao, O. Makarovsky, D. J. Walker, L. Eaves, R. I. Dykeman, S. V. Danylyuk, S. A. Vitusevich, M. J. Kappers, J. S. Barnard, and C. J. Humphreys, Phys. Status Solidi C **0**, 2389 (2003).
[6]S. Leconte, S. Golka, G. Pozzovivo, G. Strasser, T. Remmele, M. Albrecht, and E. Monroy, Phys. Status Solidi C **5**, 431 (2008).
[7]A. Kikuchi, R. Bannai, K. Kishino, C.-M. Lee, and J.-I. Chyi, Appl. Phys. Lett. **81**, 1729 (2002); **83**, 3628 (2003).
[8]S. Golka, C. Pflugl, W. Schrenk, G. Strasser, C. Skierbiszewski, M. Siekacz, I. Grzegory, and S. Porowski, Appl. Phys. Lett. **88**, 172106 (2006).
[9]E. Valcheva, K. Kirilov, B. Monemar, H. Amano, and I. Akasaki, Phys. Status Solidi C **6**, S751 (2009).
[10]C. Bayram, N. Péré-laperne, R. McClintock, B. Fain, and M. Razeghi, Appl. Phys. Lett. **94**, 121902 (2009).
[11]C. Bayram, N. Péré-Laperne, and M. Razeghi, Appl. Phys. Lett. **95**, 201906 (2009).
[12]N. Péré-Laperne, C. Bayram, L. Nguyen-Thê, R. McClintock, and M. Razeghi, Appl. Phys. Lett. **95**, 131109 (2009).
[13]C. Bayram, J. L. Pau, R. McClintock, and M. Razeghi, Appl. Phys. B: Lasers Opt. **95**, 307 (2009).
[14]C. Bayram, D. J. Rogers, F. Hosseini Teherani, and M. Razeghi, J. Vac. Sci. Technol. B **27**, 1784 (2009).
[15]H. C. Liu and D. D. Coon, J. Appl. Phys. **64**, 6785 (1988).
[16]S. Leconte, E. Monroy, and J.-M. Gerard, Superlattices Microstruct. **40**, 507 (2006).
[17]K. M. Indlekofer, E. Dona, J. Malindretos, M. Bertelli, M. Kocan, A. Rizzi, and L. Luth, Phys. Status Solidi B **234**, 769 (2002).
[18]S. N. Grinyaev and A. N. Razzhuvalov, Semiconductors **37**, 433 (2003).
[19]M. V. Petrychuk, A. E. Belyaev, A. M. Kurakin, S. V. Danylyuk, N. Klein, and S. A. Vitusevich, Appl. Phys. Lett. **91**, 222112 (2007).